

## Measurement of the Far-Infrared Magnetoconductivity Tensor of Superconducting $\text{YBa}_2\text{Cu}_3\text{O}_{7-\delta}$ Thin Films

H.-T. S. Lihn,<sup>1</sup> S. Wu,<sup>1</sup> H. D. Drew,<sup>1</sup> S. Kaplan,<sup>2</sup> Qi Li,<sup>3,\*</sup> and D. B. Fenner<sup>3</sup>

<sup>1</sup>*Department of Physics, University of Maryland, College Park, Maryland 20742*

<sup>2</sup>*Laboratory for Physical Sciences, College Park, Maryland 20740*

<sup>3</sup>*Advanced Fuel Research, East Hartford, Connecticut 06138*

(Received 10 October 1995)

We report measurements of the far-infrared transmission of superconducting  $\text{YBa}_2\text{Cu}_3\text{O}_{7-\delta}$  thin films from 5 to 200  $\text{cm}^{-1}$  in fields up to 14 T. A Kramers-Kronig analysis of the magnetotransmission spectrum yields the magnetoconductivity tensor which is found to be dominated by three terms: a London term, a low frequency Lorentzian ( $\omega_1 \approx 3 \text{ cm}^{-1}$ ) of width  $\Gamma_1 = 10 \text{ cm}^{-1}$ , and a finite frequency Lorentzian of width  $\Gamma_2 = 17 \text{ cm}^{-1}$  at  $\omega_2 = 24 \text{ cm}^{-1}$  in the hole cyclotron resonance active mode of circular polarization. [S0031-9007(96)00165-2]

PACS numbers: 74.25.Nf, 74.60.Ge, 74.72.Bk, 78.20.Ls

The electrodynamic response of type II superconductors in the mixed state is strongly affected by vortex dynamics as extensive dc transport and microwave ( $\mu$ wave) frequency studies have shown for both conventional and high temperature superconductors [1,2]. For a pinned vortex lattice the results of the  $\mu$ wave experiments can be described in terms of a conductivity function consisting of a London term, reduced from its zero field strength, and a zero frequency oscillator with a width characterized by the "depinning frequency"  $\omega_d = \kappa/\eta$  where  $\kappa$  is the pinning force constant and  $\eta$  is the viscosity [1]. In principle, however, a far richer phenomenology may be anticipated for the electrodynamics of the vortex system. The possibilities include a pinning resonance associated with the motion of the vortex in its pinning field [3], resonant excitation of quasiparticles to the quantized levels in the vortex core [4], and, in the clean limit, the collective cyclotron resonance of the electron system [5,6]. Moreover, quite generally, the response of an electron system in the presence of a magnetic field is expected to be chiral, so that  $\sigma_{xy}(\omega, H) \neq 0$ . Although evidence for these effects has not been observed at  $\mu$ wave frequencies, they have been reported from recent experiments in high  $T_c$  films at far-infrared (FIR) frequencies [5,7,8] and interpreted in terms of a clean limit theory of vortex dynamics [3]. These experiments were limited to  $\omega > 25 \text{ cm}^{-1}$  so that they did not observe the zero frequency oscillator nor did they completely resolve the pinning resonance [8]. Therefore there is a gap in our understanding of the electrodynamics of the vortex system that coincides with the frequency gap in the measurements between the  $\mu$ wave and FIR.

In this Letter we present the magnetotransmission spectrum of  $\text{YBa}_2\text{Cu}_3\text{O}_{7-\delta}$  (YBCO) films over the frequency range from 5.26 to 200  $\text{cm}^{-1}$  by using the combination of broadband Fourier transform spectroscopy (FTS) and a FIR laser source. These measurements cover the entire range of frequencies relevant to the vortex system and they

are found to provide a reconciliation of the  $\mu$ wave and FIR phenomenologies. The results show that the electrodynamic response of the pinned vortex system is dominated by two major Lorentzian oscillators in addition to a London term. These results, together with evidence of the weaker vortex core resonances reported recently [7], suggest a vortex response that combines the features of both the massless vortex model of Gittleman-Rosenblum (GR) and the clean limit model of Hsu, which includes the vortex core structure and inertia [1,3].

The samples are high quality YBCO thin films grown by pulsed laser deposition on silicon substrates with yttria stabilized zirconia buffer layers and cap layers. The film thickness is typically  $d = 400 \text{ \AA}$  and typical critical temperatures are  $T_c = 89 \pm 1 \text{ K}$  measured by ac susceptibility. Their growth and characterization is described in detail elsewhere [7,9]. The broadband transmission of the films was measured from 30 to 200  $\text{cm}^{-1}$ , using FTS with magnetic fields up to 14 T applied perpendicular to the  $a$ - $b$  plane of the YBCO. The incident FIR radiation was elliptically polarized by a polarizer comprised of a metal grid linear polarizer and a x-cut quartz wave plate. The elliptically polarized transmission data were unfolded; using a calibration of the polarizer efficiency, to give the circularly polarized response  $T^\pm(\omega, H)$ . A more detailed description of the experiment and data manipulation is given elsewhere [5,8]. For the low frequency measurements we use a  $\text{CO}_2$  pumped FIR laser which has useful discrete FIR lines from 5.26 to 96  $\text{cm}^{-1}$ . Problems with leakage of radiation and multiple reflection effects in the substrate were eliminated as described in Ref. [10].

The experiments measured both the absolute transmission at zero field  $T(\omega, 0)$  and the transmission ratio  $T^\pm(\omega, H)/T(\omega, 0)$ . The transmission coefficient  $T^\pm(\omega, H) = |t^\pm(\omega, H)|^2$  where the transmission amplitude  $t^\pm(\omega, H)$  is related to the conductivity by

$$t^\pm(\omega, H) = (n_s + 1)/[Z_0 d \sigma^\pm(\omega, H) + n_s + 1] \quad (1)$$

in which  $Z_0$  is the impedance of free space,  $n_s$  is the refractive index of the silicon substrate (nearly constant and real), and  $\sigma^\pm(\omega, H)$  is the conductivity in the two circular polarization modes. Figure 1 shows  $|t^\pm(\omega, H)/t(\omega, 0)|$  as a function of  $\omega$  at  $H = 9$  T and 4 K.  $|t(\omega, 0)|$  at 4 K is also shown in the inset. The response  $|t^+(H)/t(0)|$  in the electron cyclotron resonance active polarization (ECP) mode is plotted for positive frequencies and the hole active polarization (HCP) response  $|t^-(H)/t(0)|$  is plotted for negative frequencies. The transmission ratios show a sharp rise for  $|\omega| < 30$   $\text{cm}^{-1}$  corresponding to a peak centered in the range  $\pm 5$   $\text{cm}^{-1}$ . This low frequency feature is asymmetrical around  $\omega = 0$ ; i.e.,  $|t^-(H)/t(0)| > |t^+(H)/t(0)|$  and its field dependence is slightly super-linear. At high frequencies ( $|\omega| \geq 30$   $\text{cm}^{-1}$ ) the transmission ratio approaches unity in both modes such that  $|t^+(H)/t(0)| > 1$  and  $|t^-(H)/t(0)| < 1$  with a minimum at  $\omega \approx -40$   $\text{cm}^{-1}$ . This high frequency chiral response is found to scale linearly with magnetic field for  $H < 14$  T  $\ll H_{c2}$  [7] and has been interpreted in terms of the tail of a free holelike collective cyclotron resonance of the system [5]. The overall shape of the transmission ratio spectrum in Fig. 1 is simple, which suggests that the underlying physics of vortex electrodynamics may be very simple and elegant.

A Kramers-Kronig transformation (KKT) technique [11] is used to obtain the real and imaginary parts of the magnetoconductivity tensor as a function of frequency, which is more useful for gaining physical insight. The most convenient quantity related to the transmission

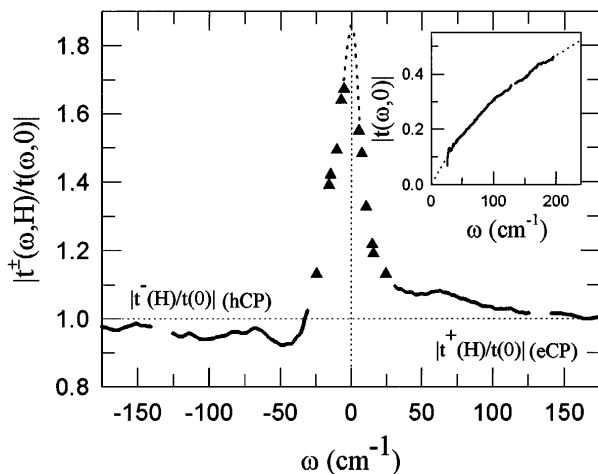


FIG. 1. The transmission amplitude ratio  $|t^{\pm}(\omega, H)/t(\omega, 0)|$  as a function of frequency  $\omega$  for a YBCO thin film at  $H = 9$  T and 4 K for circularly polarized light. The solid curve represents the FTS data from 30 to 200  $\text{cm}^{-1}$  and the triangular points represent the data from the FIR laser lines. The region between 125 and 140  $\text{cm}^{-1}$  corresponds to a quartz phonon and the half wave-plate condition of the polarizer. The dotted line is the "model extrapolation" described in text. Inset: Zero field transmission amplitude  $|t(\omega, 0)|$  vs frequency  $\omega$  at 4 K (the solid line). The dotted line is the extrapolation function  $t_{\text{ext}}(\omega)$ .

experiment that satisfies the KKT conditions is  $\ln[t(\omega)] = \ln|t(\omega)| + i\arg[t(\omega)]$  in which  $\arg[t(\omega)]$  is the phase of the complex amplitude  $t(\omega)$ . In the zero field case,  $\arg[t(\omega, 0)]$  can be obtained through KKT by properly choosing an extrapolation function  $t_{\text{ext}}(\omega)$  for  $|t(\omega, 0)|$ , which preserves time reversal symmetry (even function in  $\omega$ ) and has the correct asymptotic behavior at  $\omega \rightarrow 0$  [ $t_{\text{ext}}(\omega) \propto \omega$ ] and  $\infty$  [ $t_{\text{ext}}(\omega) \rightarrow 1$ ].  $t(\omega, 0)$  can then be converted into  $\sigma(\omega, 0)$  since  $Z_0$ ,  $d$ , and  $n_s$  are known. Detailed analysis shows that the film consists of  $f_{s,0} = 0.61$  of superfluid condensate with the London penetration depth  $\lambda_0 = 1850$   $\text{\AA}$  [12].  $\text{Re}[\sigma(\omega, 0)]$  is shown in the inset to Fig. 2.

When a magnetic field is applied to the system, time reversal symmetry is broken and it becomes necessary to determine the proper response function for both positive and negative frequencies. In this case, the two circularly polarized modes are the canonical modes. We can extend any response function  $g^+(\omega, H)$  to the negative frequency range by

$$g^+(\omega, H) \equiv \begin{cases} g^+(\omega, H), & \text{when } \omega > 0 \text{ (ECP)}, \\ g^-(-\omega, H)^*, & \text{when } \omega < 0 \text{ (HCP)}, \end{cases} \quad (2)$$

where  $g^\pm(\omega, H)$  are the physical quantities measured for positive frequencies in the two circularly polarized modes. Thus the KKT for the magnetic field case becomes

$$\arg\left[\frac{t^+(\omega, H)}{t(\omega, 0)}\right] = \frac{1}{\pi} P \int_{-\infty}^{\infty} \frac{\ln|t^+(\omega', H)/t(\omega', 0)|}{\omega - \omega'} d\omega'. \quad (3)$$

By combining this with  $\sigma(\omega, 0)$ , we can obtain  $\sigma^+(\omega, H)$  ( $-\infty < \omega < \infty$ ) and therefore  $\sigma^\pm(\omega, H)$  ( $0 < \omega < \infty$ ).

Figure 2 shows the magnetoconductivity  $\text{Re}[\sigma^+(\omega, H)]$  obtained by KKT on the transmission curves in Fig. 1 with a "model extrapolation" scheme for

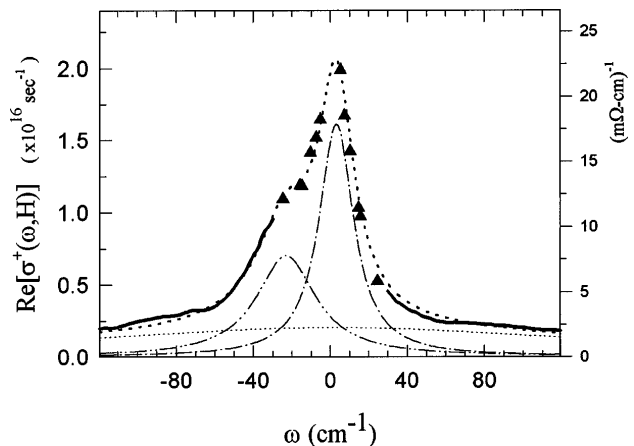


FIG. 2. The magnetoconductivity  $\text{Re}[\sigma^+(\omega, H)]$  obtained from the Kramers-Kronig analysis. The change induced by the magnetic field can be described as the sum (dotted line) of a low frequency oscillator of width  $\Gamma_1 = 10$   $\text{cm}^{-1}$  at  $\omega_1 = +3.15$   $\text{cm}^{-1}$  (single dot-dashed line) and an oscillator of width  $\Gamma_2 = 17$   $\text{cm}^{-1}$  at  $\omega_2 = -24$   $\text{cm}^{-1}$  (double dot-dashed line). The small dotted line is  $\text{Re}[\sigma(\omega, 0)]$ .

$|\omega| < 5 \text{ cm}^{-1}$ , which will be described below. Apart from the residual metallic background which is present in  $\text{Re}[\sigma(\omega, 0)]$  [12], the conductivity function evolves from its zero field London form  $[(ne^2/m)f_{s0}i/\omega]$  into a form with a reduced London component and several finite frequency absorption bands, which can be well represented as a finite sum of Lorentzian oscillators  $\sigma_H(\omega, H) = (ne^2/m)\sum_{i=0}^M f_i/[i(\omega - \omega_i) + \Gamma_i]$  where  $f_i$  represents the strength of the  $i$ th oscillator. Indeed, two finite width oscillators ( $M = 2$ ) in addition to a reduced strength London term ( $\omega_0 = 0, \Gamma_0 = 0$ ) is sufficient to describe the main features induced by vortex dynamics. The best fit with  $M = 2$  is shown as the dotted line in Fig. 2. The first oscillator is at low frequency ( $\omega_1 = 3.15 \text{ cm}^{-1}$ , in ECP mode) with  $f_1 = 0.14$  (23% of  $f_{s0}$ ) and a width  $\Gamma_1 = 10 \text{ cm}^{-1}$  [13] which is similar to the form of the GR model [1]. The second oscillator is centered at  $\omega_2 = -24 \text{ cm}^{-1}$  (in the HCP mode) with  $f_2 = 0.11$  (18% of  $f_{s0}$ ) and a width  $\Gamma_2 = 17 \text{ cm}^{-1}$ , which produces the optical activity observed at higher frequencies [8]. The remaining oscillator strength gives  $f_0 = 0.36$  (59% of  $f_{s0}$ ) since  $f_0 + f_1 + f_2 = f_{s0}$ .

The superfluidity of the condensed state leads to a special sum rule on  $t(\omega)$ . For pinned type II superconductors the superfluid condensate response causes the low frequency conductivity to be dominated by the London screening,  $\sigma(\omega \rightarrow 0) \sim i/\omega + \pi\delta(\omega)$ . Therefore  $t^+(0, H)/t^-(0, 0)$  is the ratio of the strength of two delta functions which is a real number (for  $H < H_{c2}$ ). The left hand side of Eq. (3) is zero (when  $\omega \rightarrow 0$ ) which leads to the relation

$$\int_0^\infty \ln |t^+(\omega, H)/t^-(\omega, H)| \frac{d\omega}{\omega} = 0. \quad (4)$$

This sum rule provides a strong constraint on the magnetotransmission data which is useful for setting the extrapolations in the KKT analysis. Figure 3 shows  $|t^+(\omega, H)/t^-(\omega, H)|$  as a function of  $\ln(\omega)$  and the integral weight of Eq. (4) in the various frequency ranges. Assuming that free hole behavior eventually dominates the free carrier response at sufficiently high frequencies, then  $\ln |t^+/t^-|/\omega \sim \omega_c/\omega^4\tau$ , which indicates a strongly convergent (or superconvergent) sum rule. Indeed, extrapolation of the broadband data by the cyclotron resonance model suggests that the frequency range beyond  $190 \text{ cm}^{-1}$  contributes only about 10% to the integral. We have also confirmed the observation of a sign reversal of the optical activity ( $T^+/T^- - 1$ ) in YBCO films [8] (the same batch of samples as in this Letter) at about  $30 \text{ cm}^{-1}$ . Remarkably, this feature is seen to be a natural consequence of Eq. (4).

Even though several different extrapolation schemes based on reasonable physical assumptions in the unmeasured regions ( $|\omega| < 5.26 \text{ cm}^{-1}$  and  $|\omega| > 200 \text{ cm}^{-1}$ ) give similar results and preserve the two oscillator picture of the conductivity, the use of Eq. (4) allows a refine-

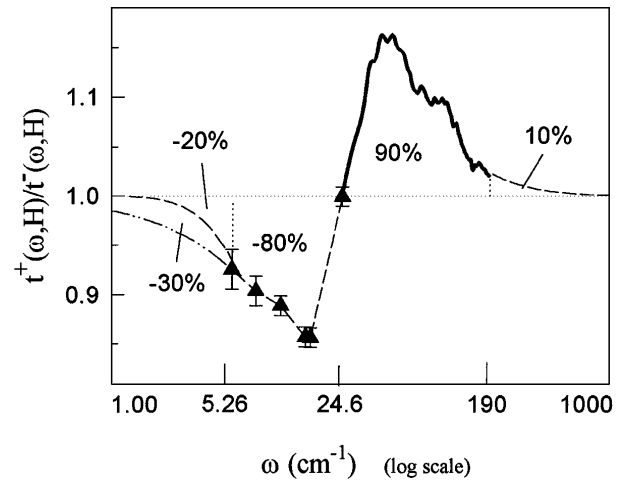


FIG. 3.  $|t^+(\omega, H)/t^-(\omega, H)|$  is plotted as a function of  $\ln(\omega)$ . The spectral weights of different frequency regions to the sum rule of Eq. (4) are indicated. The dashed line between laser data points is a guide for the eye. The double dot-dashed line is the simple cubic spline extrapolation which behaves as  $\ln |t^+/t^-| \sim \omega$  below  $5 \text{ cm}^{-1}$ . The dashed line is the “model extrapolation” which satisfies the sum rule.

ment of the analysis. A simple cubic spline interpolation in the range  $\pm 5.26 \text{ cm}^{-1}$  gives  $\ln |t^+/t^-| \sim \omega$ , which results in  $\sim 30\%$  excess weight in the low frequency region compared to the high frequency region (double dot-dashed line in Fig. 3). There are two possible resolutions of this discrepancy. The first possibility is that there are other (electronlike) chiral resonances in addition to the simple cyclotron resonance tail above  $200 \text{ cm}^{-1}$  which balances the low frequency weight. Simulations show that an additional 7% mid-IR chiral resonance at  $\sim 500 \text{ cm}^{-1}$  will allow the sum rule to be satisfied. However, this resonance would cause the optical activity to change sign twice below  $500 \text{ cm}^{-1}$  and there has been no evidence for this in our measurements up to  $200 \text{ cm}^{-1}$  [8]. The second possibility is that  $\ln |t^+/t^-|$  decreases faster than  $\omega$  at low frequencies (below  $5 \text{ cm}^{-1}$ ). By using the two Lorentzian model mentioned above for the model extrapolation and shifting the low frequency oscillator to  $\omega_1 > 0$  (electronlike) we find that the sum rule can be satisfied (dashed line below  $5 \text{ cm}^{-1}$ ).

Figure 4(a) shows the resulting  $\text{Im}[\sigma_{xx}(\omega, H)]/\text{Im}[\sigma(\omega, 0)]$ , which describes the modification of the screening in the applied field. This ratio approaches 0.55 as  $\omega \rightarrow 0$ . In terms of the G-R model [1]  $\text{Im}[\sigma_{xx}(0, H)]/\text{Im}[\sigma(0, 0)] = \kappa/[\kappa + (c^2/\mu)]$  gives  $\kappa \approx 5.3 \times 10^5 \text{ N/m}^2$ , which is consistent with diverse  $\mu$ wave measurements [2,13]. The resonance at  $24 \text{ cm}^{-1}$  is seen in  $\sigma_{xy}$  in Figs. 4(b) and 4(c). According to the sum rule the contributions of this resonance and the low frequency oscillator to  $\text{Re}[\sigma_{xy}]$  at  $\omega = 0$  nearly cancel leading to a suppressed Hall effect at low frequencies [Fig. 4(b)]. There are additional smaller structures (for  $\omega > 50 \text{ cm}^{-1}$ ) in the conductivity, many of which are

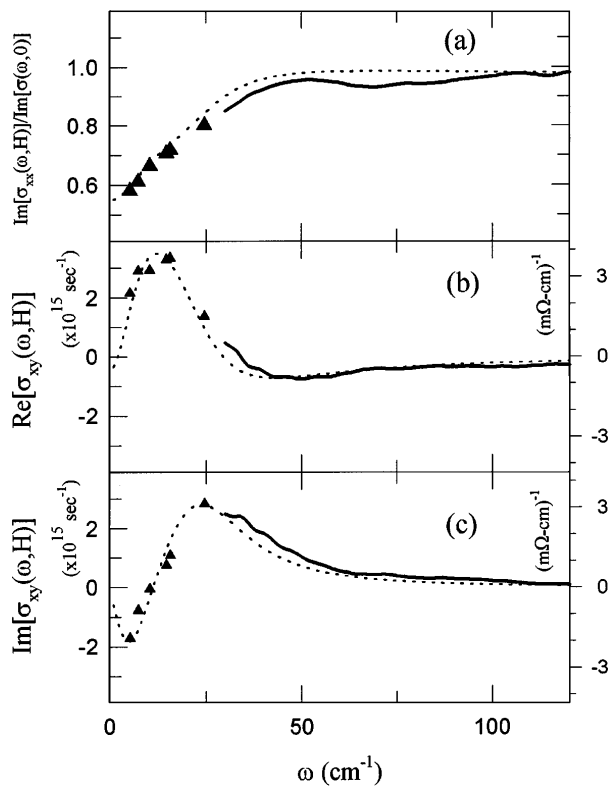


FIG. 4. The magnetoconductivity is shown in the Cartesian representation,  $\sigma_{xx}$  and  $\sigma_{xy}$ . The dotted lines are the two Lorentzian model fits described in Fig. 2.

found to correlate with the density of  $45^\circ$  misaligned grains in the samples. They have been discussed elsewhere in terms of vortex core excitations [7].

Within the GR type models optical activity and the nonzero center frequency of the low frequency oscillator implies that a Hall force must be added to the Lorentz force leading to  $ne(v_s - \beta v_L)\phi_0$  where  $\beta \approx -0.1$  characterizes the Hall term [14]. The negative  $\beta$  is consistent with the observation of a reversal of dc Hall effect in the flux flow regime [15]. In the GR model optical activity requires a Hall force, but the zero vortex mass keeps the resonance at low frequency. On the other hand Hsu's model contains a Magnus force ( $\beta = 1$ ), core excitations, and, implicitly, a vortex mass. This produces two finite frequency chiral resonances. In the absence of pinning the Hsu model predicts that the core resonance is silent and that the response of the superconductor is a collective resonance as expected from Kohn's theorem [6]. Pinning hybridizes the cyclotron resonance and vortex core resonance with the pinning resonance. The result is a strong hybridized pinning resonance at a negative frequency, which gives optical activity and a weak hybridized vortex core resonance at a positive frequency.

The observed response is seen to contain the features of both theories, but is inconsistent with either one alone. It appears that there is a massless response of the vortices

that gives rise to the low frequency oscillator in addition to a finite vortex mass response that gives rise to the pinning resonance and the weak vortex core resonance [7,8]. These observations suggest a model in which the vortex is considered as a composite object consisting of massless vortex currents and a massive core with its quantum structure. A paper describing this model will be presented elsewhere [14].

The authors acknowledge helpful discussions with V. Yakovenko and F. Wellstood. This work is supported by the NSF under Grant No. DMR9223217. The work at Advanced Fuel Research was supported by Contract No. DOE-SBIR (No. DE-FG01-90ER81084 and No. DE-FG05-93ER81507).

\*Present address: Applied Materials, Santa Clara, CA 95050.

- [1] J. I. Gittleman and B. Rosenblum, Phys. Rev. Lett. **16**, 734 (1966); M. W. Coffey and J. R. Clem, Phys. Rev. Lett. **67**, 386 (1991).
- [2] M. Golosovsky *et al.*, Phys. Rev. B **50**, 470 (1994); S. Revenaz *et al.*, Phys. Rev. B **50**, 1178 (1994).
- [3] T. C. Hsu, Physica (Amsterdam) **213C**, 305 (1993).
- [4] Y. Zhu, F. Zhang, and H. D. Drew, Phys. Rev. B **47**, 586 (1993); B. Janko and J. Shore, Phys. Rev. B **46**, 9270 (1992).
- [5] K. Karrai *et al.*, Phys. Rev. Lett. **69**, 355 (1992).
- [6] H. D. Drew and T. C. Hsu, Phys. Rev. B **52**, 9178 (1995).
- [7] H.-T. S. Lihn *et al.*, Phys. Rev. B **53**, 1 (1996).
- [8] E.-J. Choi *et al.*, Phys. Rev. B **49**, 13271 (1994); E.-J. Choi *et al.*, Physica (Amsterdam) **254C**, 258 (1995).
- [9] D. K. Fork *et al.*, Appl. Phys. Lett. **57**, 1161 (1990).
- [10] S. Wu *et al.* (to be published).
- [11] L. D. Landau and E. M. Lifshitz, *Electrodynamics of Continuous Media* (Addison-Wesley, Reading, MA, 1960).
- [12]  $\sigma(\omega, 0)$  can be represented very well by a sum of three components,  $(ne^2/m)f_{s0}i/\omega + f_{m1}\sigma_{m1} + f_{m2}\sigma_{m2}$ : (1) superfluid condensate,  $f_{s0} = 0.61$ ; (2) normal metal,  $f_{m1} = 0.28$  and  $\sigma_{m1} = (ne^2/m)/(-i\omega + 1/\tau)$  with  $1/\tau = 150 \text{ cm}^{-1}$ ; and (3) a nearly frequency independent normal component (over the measured frequency range),  $f_{m2} = 0.11$  and  $\sigma_{m2} = (ne^2/m)/(-i\omega + 1/\tau)$  with  $1/\tau \approx 600 \text{ cm}^{-1}$ . The total oscillator strength is given by  $4\pi ne^2/m = c^2/\lambda_0^2$ , which corresponds to  $\lambda_0 = 1850 \text{ \AA}$ . The strength of the Drude components is found to be sample dependent. The second term is believed to represent superconducting dead layers at the interfaces of the YBCO films and the third term is related to either the mid-IR contributions [16] or the chain conductivity in YBCO. Both terms are believed to be field independent.
- [13] B. Parks *et al.*, Phys. Rev. Lett. **74**, 3265 (1995).
- [14] H.-T. S. Lihn and H. D. Drew (unpublished); Report No. cond-mat/9601142 (to be published).
- [15] A. T. Dorsey, Phys. Rev. B **46**, 8376 (1992); S. J. Hagen *et al.*, Phys. Rev. B **47**, 1064 (1993).
- [16] K. Kamaras *et al.*, Phys. Rev. Lett. **64**, 84 (1990).